COLLÈGE DE FRANCE
1530

Chaire de Physique de la Matière Condensée

Des oxydes supraconducteurs aux atomes froids

- la matière à fortes corrélations quantiques -

Antoine Georges

Cycle 2009-2010
Cours 4 - 26 mai 2010

Cours 4: Quasiparticules et Liquides de Fermi

Séminaire:

COLLÈGE DE FRANCE 1530

Henri GODFRIN

Institut Néel, CNRS, Grenoble

L'Helium-3 liquide bidimensionnel: un liquide de Fermi fait pour intriguer les physiciens !

La phase liquide de l'hélium-3 est un système modèle d'atomes en interaction permettant l'étude de la matière condensée obéissant à la statistique quantique de Fermi-Dirac, l'un des grands problèmes de la physique actuelle. On sait réaliser des liquides de Fermi *bidimensionnels* en adsorbant des atomes d'hélium-3 sur un substrat de graphite. Leur étude très récente par des techniques neutroniques a permis d'observer que des excitations élémentaires bien définies peuvent survivre à des énergies et vecteurs d'onde élevés. Cette découverte pourrait avoir des conséquences importantes dans un domaine plus vaste et riche en applications, celui des systèmes électroniques fortement corrélés, notamment les supraconducteurs à haute température critique.

Outline:

- Motivations/Phenomenology – some classic examples
- Quasiparticles and the (N+1)-body problem
- Quasiparticles and Green's function
- Probing quasiparticles by photoemission
- Why are quasiparticles long-lived: phase-space constraints
- Landau theory of Fermi liquids
- The RG viewpoint

1. Motivations

- Quantum fluids of interacting fermions often display, at low enough temperature, physical properties which are qualitatively similar to those of a free Fermi gas.
- For example:

- Specific heat linear in temperature $C \sim \gamma T$
- Constant (Pauli-like) susceptibility χ

- *However, quantitative changes from free gas, e.g.* γ/γ_0 χ/χ_0 *can be very large.*
- *Also, deviations found as temperature is increased*

1.1 Helium 3: the historical prototype of a Fermi liquid

- For many decades, this has been the ~ only available Fermi liquid available in the lab w/out the additional complications of partially broken translation invariance due to crystal lattice as for electron gases in solids.
- [Aside from neutron stars…]
- A byproduct of the Manhattan project ! → no surprise focus was in the early 50's (cf. JG Daunt, Science, 26 Feb 1960)

* Situation now changed with cold gases of fermionic atoms (^{6}Li, ^{40}K)

Helium3 : phase diagram

Solifidification: ~ 34 bars ; Pomeranchuk minimum
Remains a liquid down to T=0 (`normal' above a few mK)

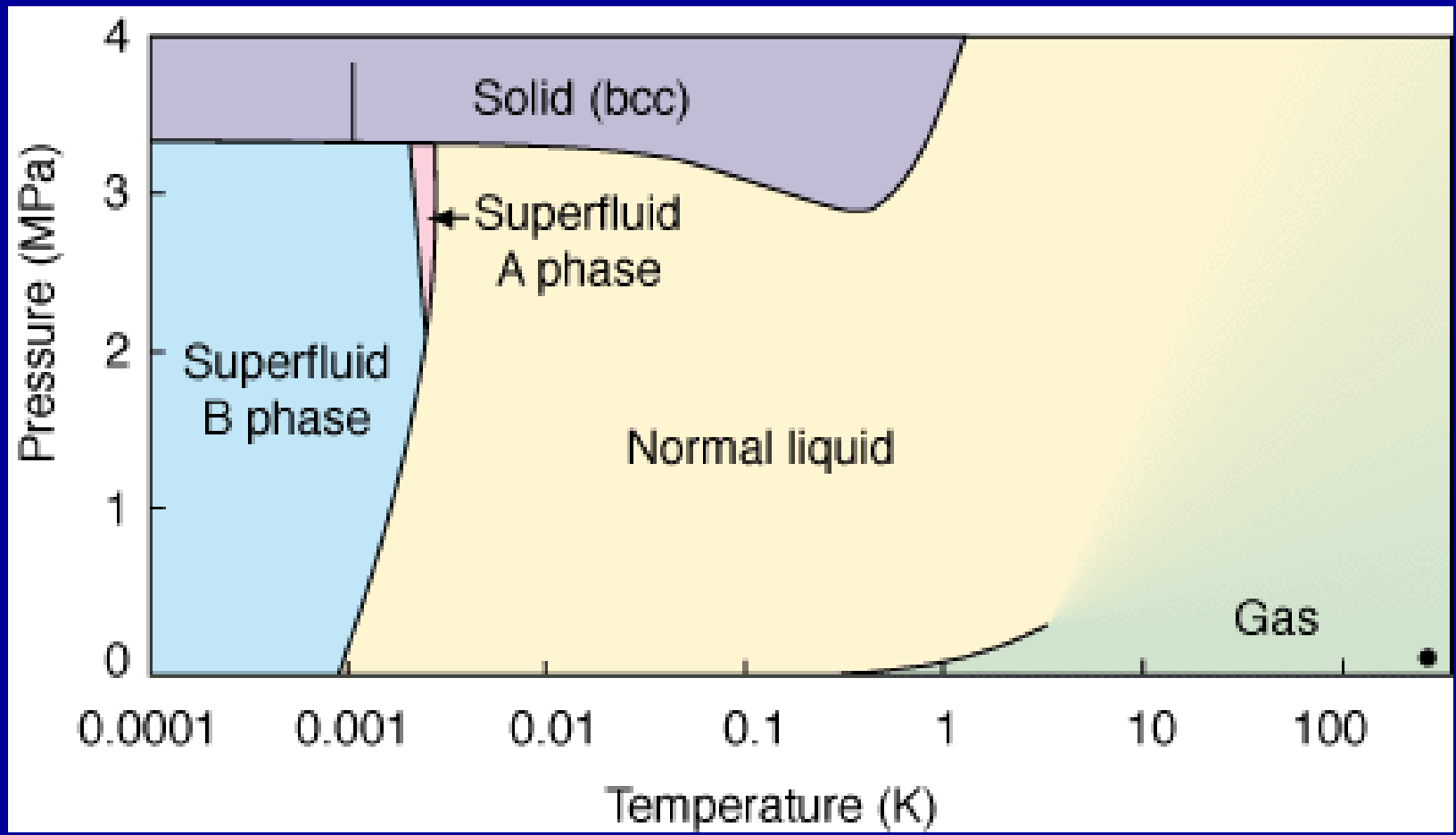

Helium 3: specific heat

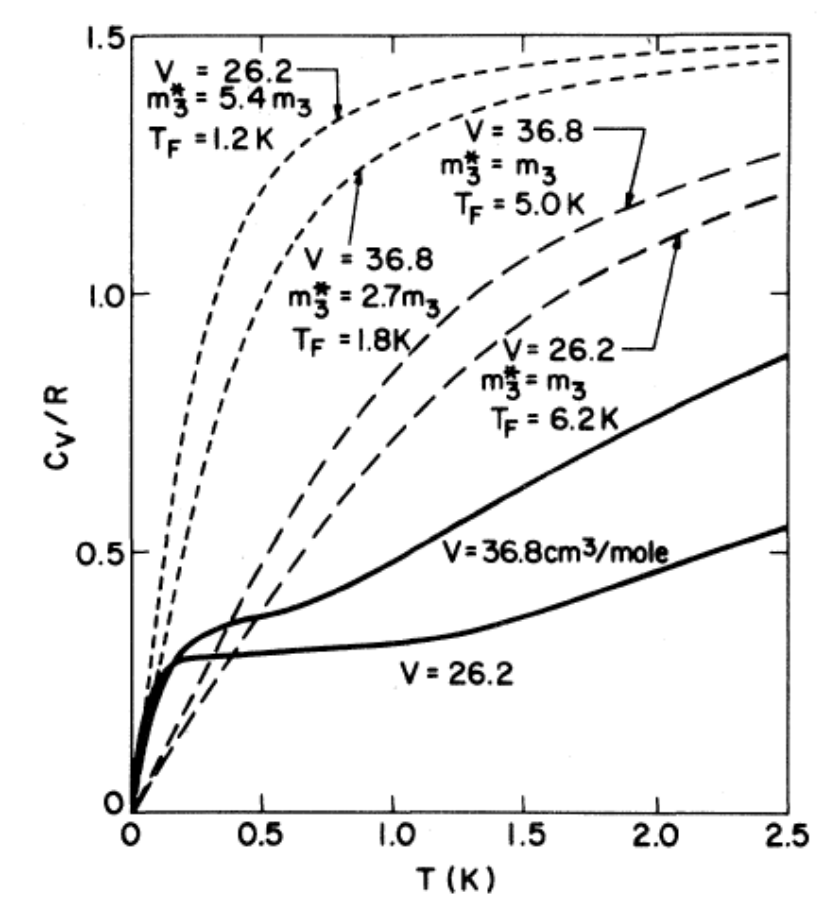

FIG. 6. Smoothed results for the ^{3}He specific heat (in units of the gas constant R) measured at molar volumes corresponding to nominal sample pressures of 0 and 29 bar. For comparison, long-dashed curves show the ideal-Fermi-gas specific heat at the same two densities. Short-dashed curves were also computed using the ideal-gas relations but with the particle mass adjusted to give the correct limiting slopes at $T = 0$.

DS Greywall,
Phys Rev B 27 (1983) 2747

-T-linear at low-T
- Slope enhanced from ~ 3 (p=0) to ~ 6 (p ~ p_s)
- Plateau at ~ 300 mK

(compare T_F gas ~ 5K at p=0)

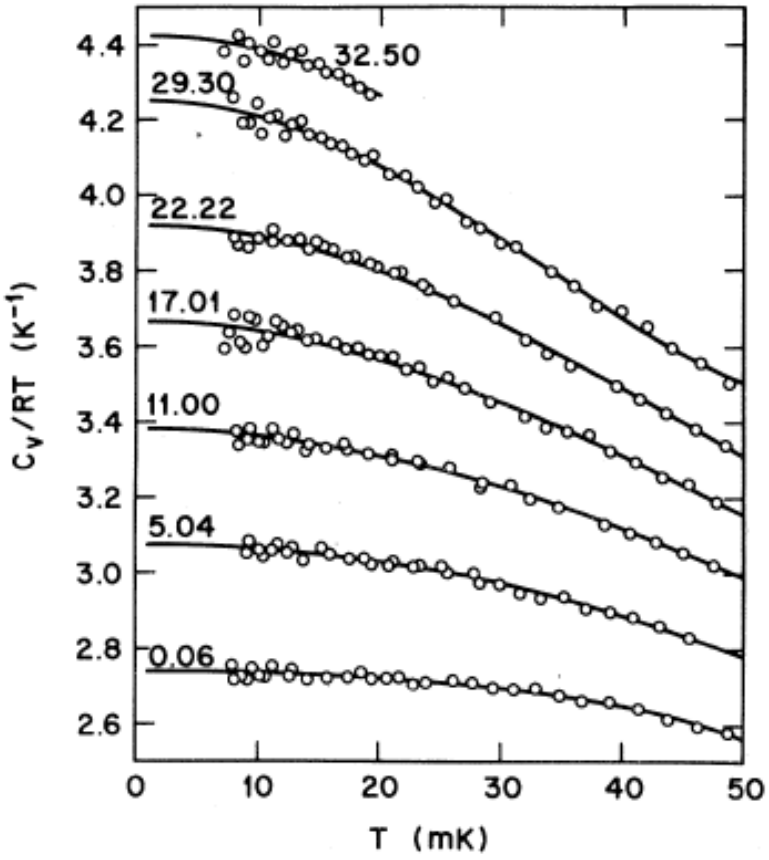

FIG. 14. Specific-heat measurements plotted as C_V/RT vs T. Numbers give the sample pressures in bars at 0.1 K. Solid curves are least-squares fits of the data using Eq. (11).

Effective degeneracy temperature << T_F^0 :

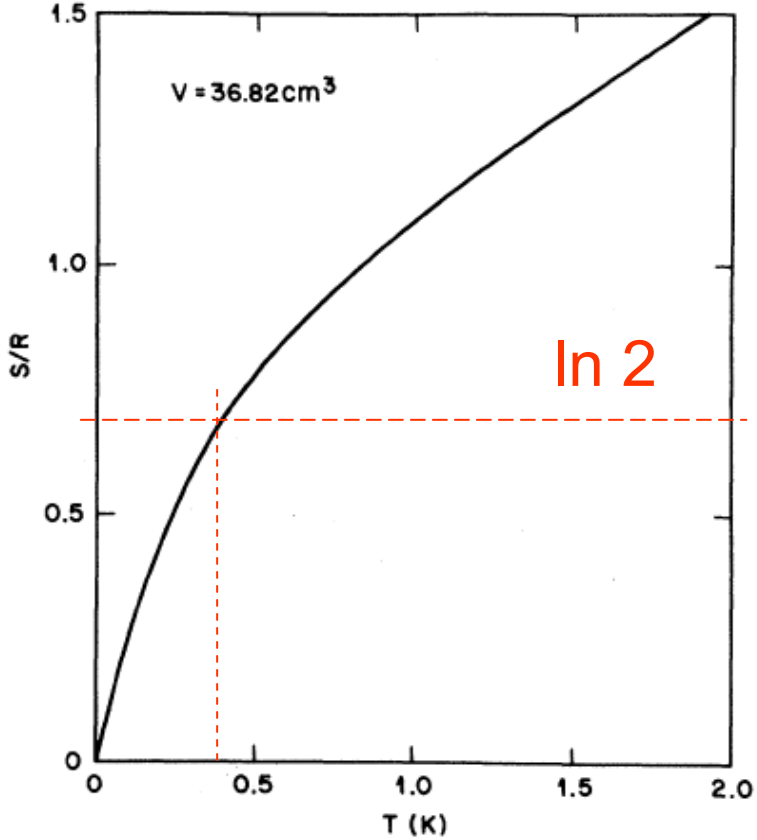

FIG. 10. ^{3}He entropy at a molar volume of 36.82 cm^3.

T=0 comparison to free gas

	Specificheat $\gamma/\gamma_0 = m^*/m$	Susceptibility $\chi/\chi_0 = \frac{m^*/m}{1+F_0^a}$	Compressibility $\kappa/\kappa_0 = \frac{m^*/m}{1+F_0^s}$
$p = 0$	2.8	9.2	0.27
$p \simeq p_s$	5.8	24	0.066

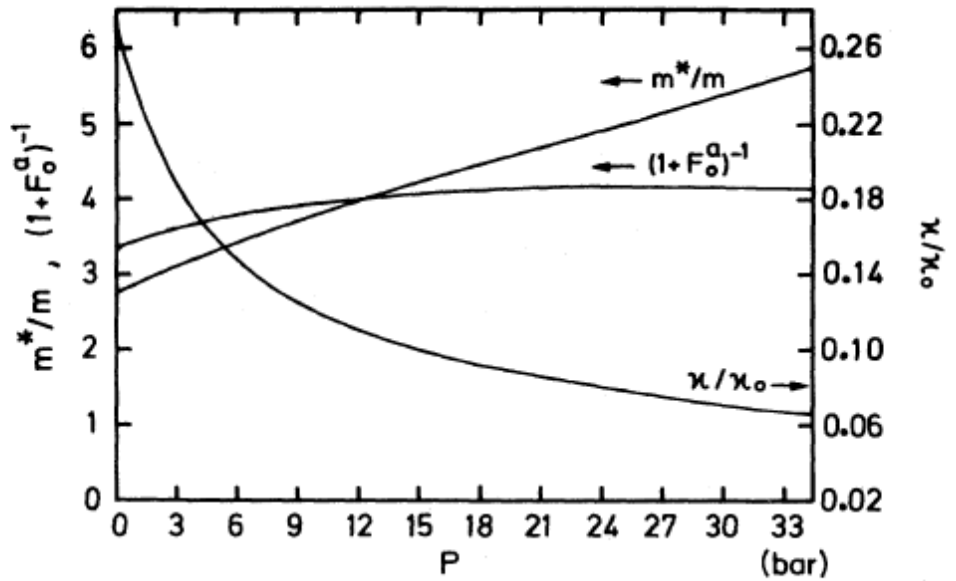

FIG. 1. Experimental values (Greywall, 1983) of the normalized effective mass m^*/m, the ratio between spin susceptibility and effective mass, $(1+F_0^a)^{-1}$, and the normalized compressibility κ/κ_0.

From D.Vollhardt Rev Mod Phys, 1984

1.2 Heavy fermion compounds:

enormous renormalizations,
robustness of Fermi liquid theory !

4*f*-Virtual-Bound-State Formation in $CeAl_3$ at Low Temperatures

K. Andres and J. E. Graebner
Bell Laboratories, Murray Hill, New Jersey 07974

Phys Rev Lett 35 (1975) 17779

and

H. R. Ott
Laboratorium für Festkörperphysik, Eidgenössische Technische Hoc
Hönggerberg, Zürich, Switzerland

(Received 25 August 1975)

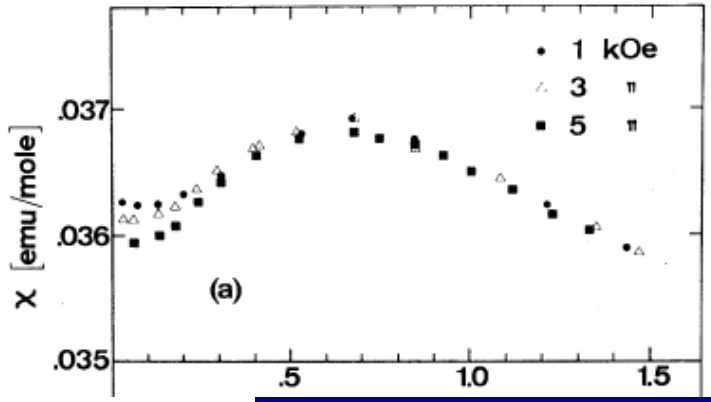

Specific-heat and electrical-resistivity measurements in $CeAl_3$ below 0.2 K reveal enormous magnitudes of the linear specific-heat term $C=\gamma T$ ($\gamma=1620$ mJ mole/K^2) and the T^2 term in $\rho=AT^2$ ($A=35$ $\mu\Omega$ cm/K^2). We conclude that the 4*f* electrons obey Fermi statistics at low temperatures because of the formation of virtual bound 4*f* states.

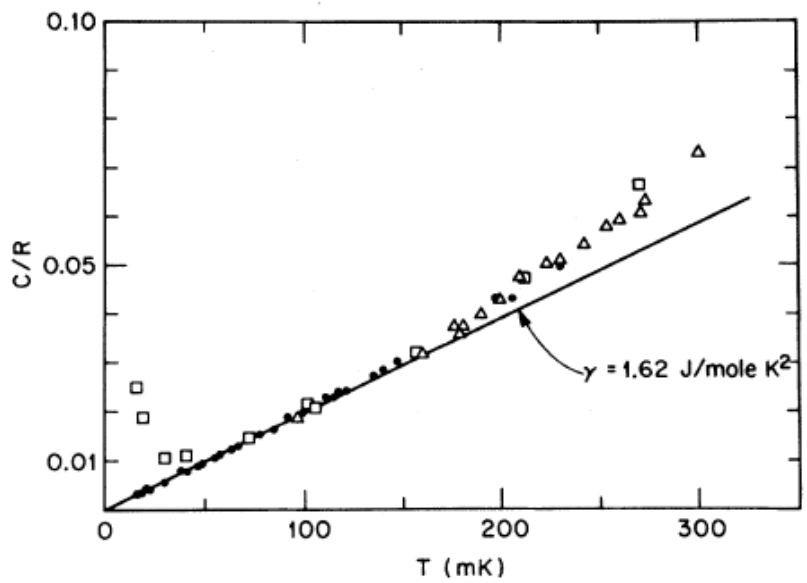

FIG. 1. Specific heat of $CeAl_3$ at very low temperatures in zero field (●, Δ) and in 10 kOe (□).

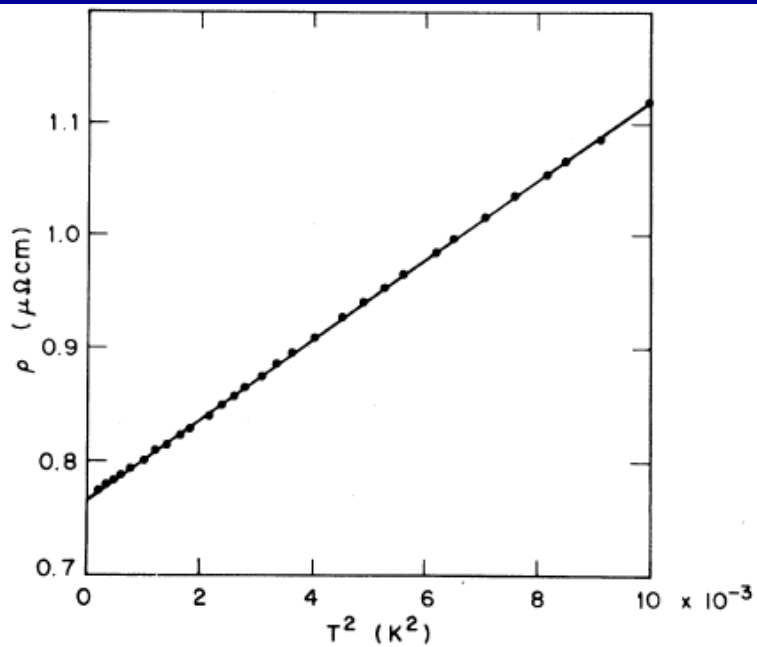

FIG. 3. Electrical resistivity of $CeAl_3$ below 100 mK, plotted against T^2.

Probing quasiparticles by angular-resolved photoemission spectroscopy (ARPES)

- Introductory review:
- A.Damascelli Phys.Scripta T109 (2004) 61

http://www.physics.ubc.ca/~quantmat/ARPES/PEOPLE/damascelli.html

Schematic view of an ARPES measurement:

A. Damascelli, Z. Hussain, Z.-X Shen, Rev. Mod. Phys. **75**, 473 (2003)

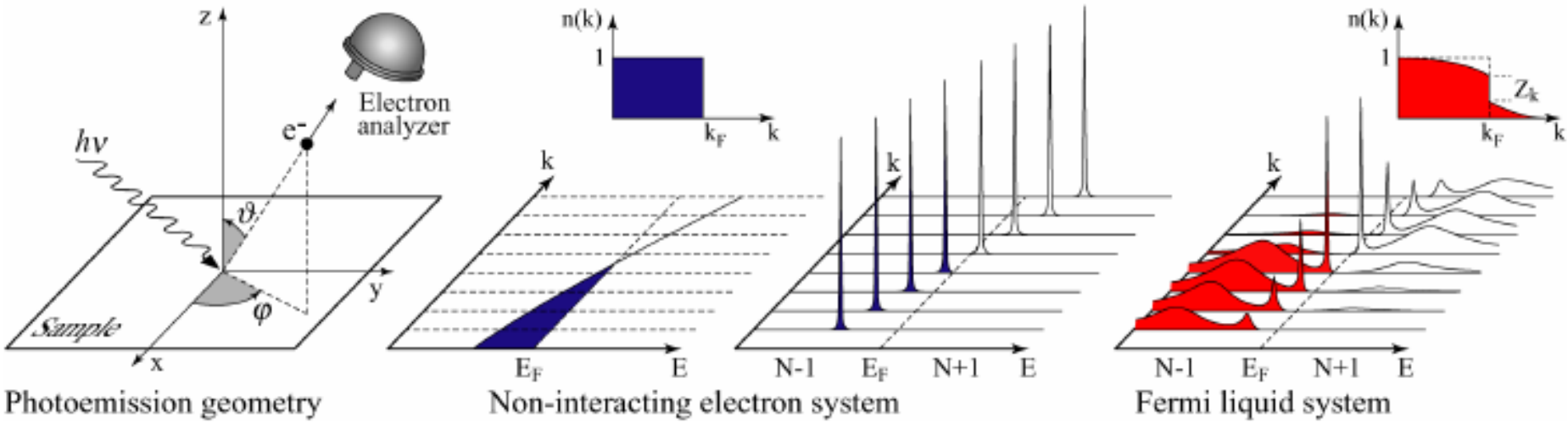

Photoemission intensity: $I(\mathbf{k}, E_{kin}) = \sum_{f,i} w_{f,i}$

$$I(\mathbf{k}, E_{kin}) \propto \sum_{f,i} |M^{\mathbf{k}}_{f,i}|^2 \sum_{m} |c_{m,i}|^2 \delta(E_{kin} + E^{N-1}_m - E^N_i - h\nu)$$

$$|M^{\mathbf{k}}_{f,i}|^2 \equiv |\langle \phi^{\mathbf{k}}_f | \mathbf{A}\cdot\mathbf{p} | \phi^{\mathbf{k}}_i \rangle|^2 \qquad |c_{m,i}|^2 = |\langle \Psi^{N-1}_m | \Psi^{N-1}_i \rangle|^2$$

In general $\Psi^{N-1}_i = c_{\mathbf{k}} \Psi^N_i$ NOT orthogonal Ψ^{N-1}_m

Photoemission intensity: $I(k,\omega)=I_0\,|M(k,\omega)|^2 f(\omega)\,A(k,\omega)$

Single-particle spectral function

$$A(\mathbf{k},\omega)=-\frac{1}{\pi}\frac{\Sigma''(\mathbf{k},\omega)}{[\omega-\epsilon_{\mathbf{k}}-\Sigma'(\mathbf{k},\omega)]^2+[\Sigma''(\mathbf{k},\omega)]^2}$$

$$A^{\pm}(\boldsymbol{k},\omega)=\sum_m |\langle\Psi_m^{N\pm1}|c_{\boldsymbol{k}}^{\pm}|\Psi_i^N\rangle|^2\,\delta(\omega-E_m^{N\pm1}+E_i^N)$$

In practice …

SSRL Beamline 5-4 : NIM / Scienta System

STANFORD SYNCHROTRON RADIATION LABORATORY

SSRL

- **High resolution**

ΔE (meV)	$\Delta\theta$
2-10	0.2°

- Ultra-high vacuum (~ 10^{-11} torr)
- High angular precision (+/- 0.1°)
- Low base temperature (< 10 K)
- Wide temperature range (10-350 K)
- Variable photon energies (12-30 eV)
- Multiple light sources (He lamp)
- Control of light polarization
- Single crystal cleaving tools
- Sample surface preparation & cleaning
- Low-Energy Electron Diffraction (LEED)

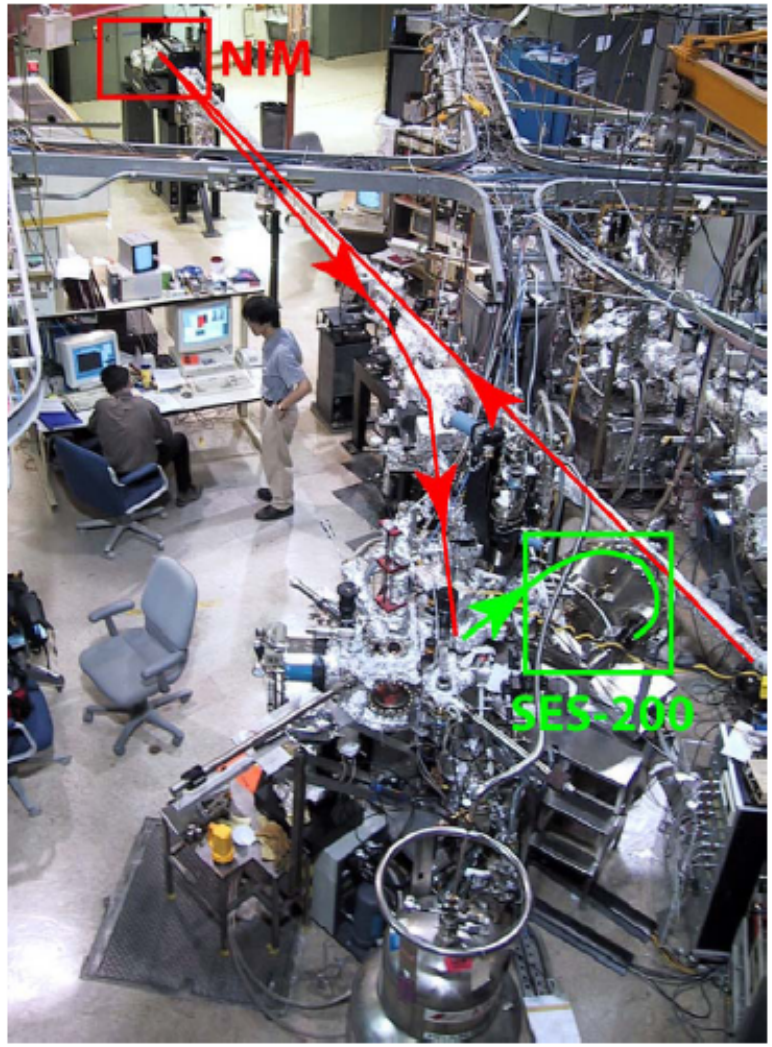

Quasiparticles:

waves associated w/ low-energy excitations
acquire a finite lifetime
(Landau Fermi-liquid theory)

Long-lived excitations with:

-Dispersion relation modified by interactions $\xi_{\mathbf{k}}$

-Finite spectral weight $Z_{\mathbf{k}}$

- Finite lifetime $\Gamma_{\mathbf{k}}^{-1}$

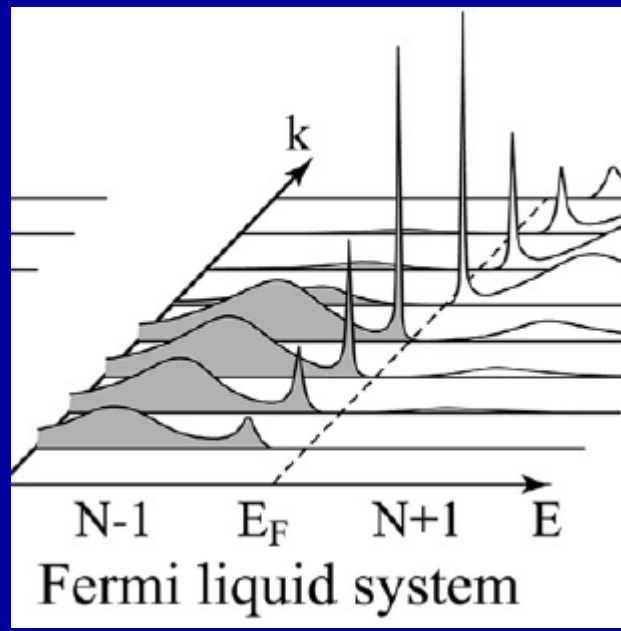

$$A(\mathbf{k},\omega) = \sum_n |\langle \Psi_n^{N-1}|\psi_{\mathbf{k}}|\Psi_0^N\rangle|^2\,\delta(\omega+\mu+E_n-E_0)$$

$$A = A_{\mathrm{QP}} + A_{\mathrm{inc}}$$

$$A_{\mathrm{QP}}(\mathbf{k},\omega) \simeq Z_{\mathbf{k}} \frac{\Gamma_{\mathbf{k}}}{\pi[(\omega-\xi_{\mathbf{k}})^2+\Gamma_{\mathbf{k}}^2]}$$

Landau: lifetime diverges as 1/(energy)^2 as FS is reached

ARPES on `model' systems
- quantitative analysis of lineshape -

- TiTe2 (2D metal w/ weak-moderate correlations)

- Claessen et al. PRL 69 (1992) 2008; PRB 54 (1996) 2453; PRB 74 (2006) 195125
- Perfetti et al. PRB 64 (2001) 115102

- Mo(110) surface state

- T.Valla et al. PRL 83 (1999) 2085

- Sr_2RuO_4

- Ingle et al. PRB 72 (2005) 205114
- Wang et al PRL 92 (2004) 137002
- Kidd et al. PRL 94 (2005) 107003

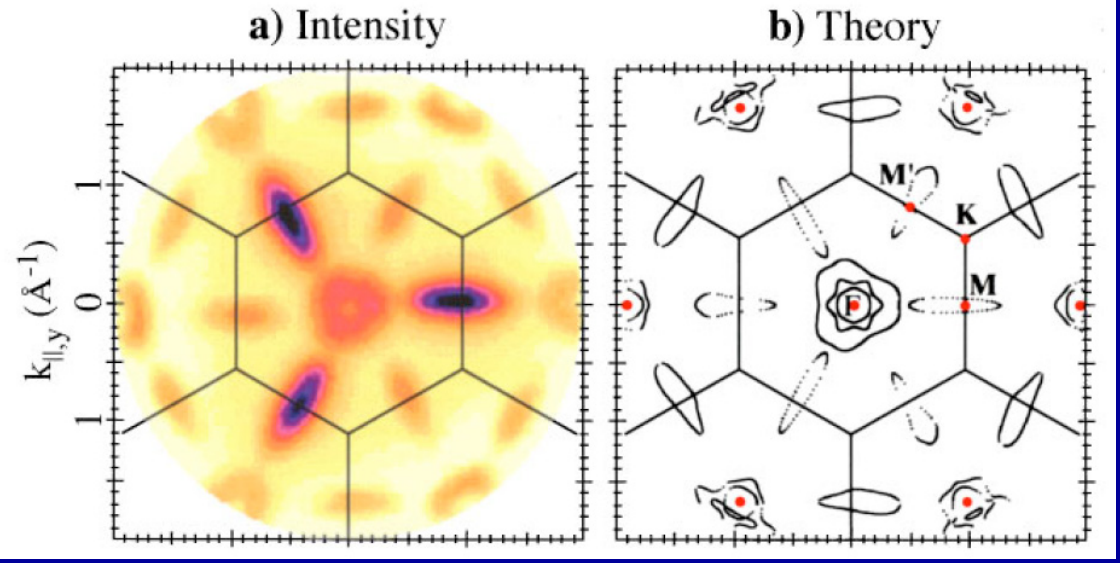

$$\mathrm{Im}\Sigma_{e\text{-}ph}(T,\omega)=\pi\int_0^\infty d\nu\alpha^2F(\nu)[2n(\nu)+f(\nu+\omega)+f(\nu-\omega)].$$

$$\alpha^2F(\omega)=\lambda(\omega/\Omega_m)^2$$

$$\Sigma_{e\text{-}e}(\omega)=\alpha\omega+i\beta[\omega^2+(\pi k_BT)^2].$$

$$\beta=0.7\pm0.2\ \ \mathrm{eV}^{-1}$$

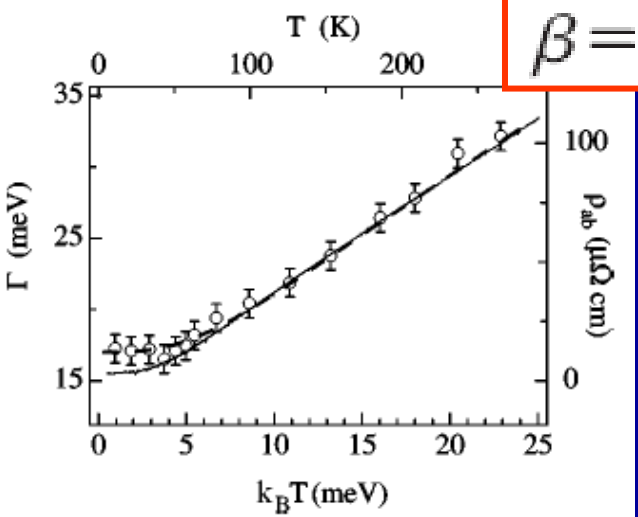

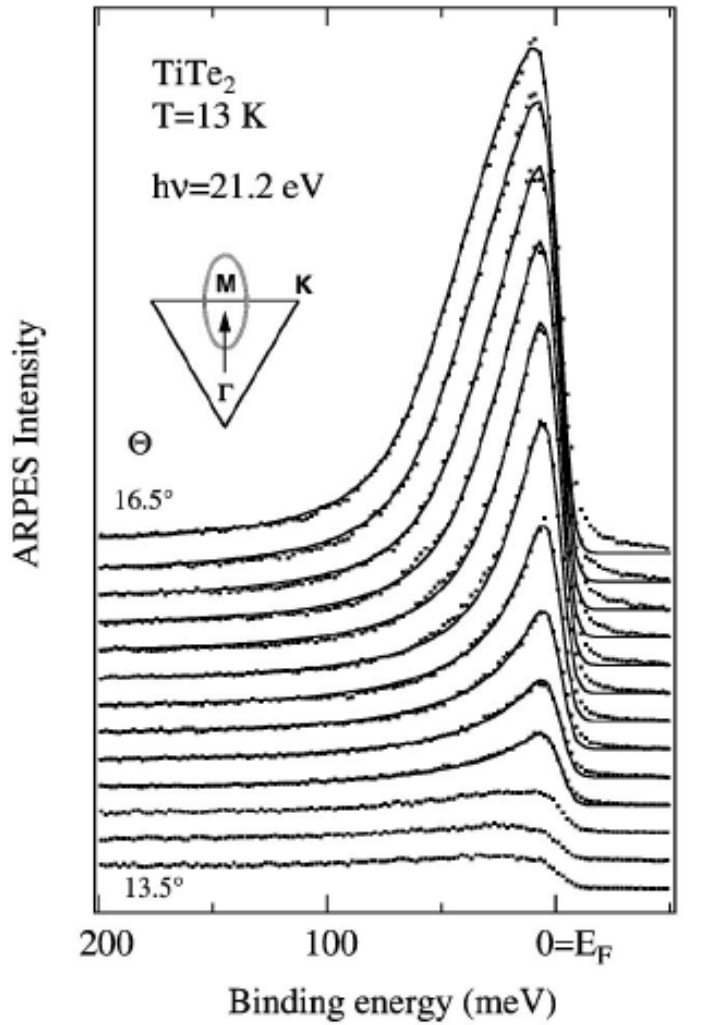

FIG. 1. High-resolution ARPES spectra of 1T-TiTe$_2$ measured near the Fermi surface crossing along the high-symmetry ΓM direction ($\theta=0$ is normal emission). The lines are the results of Fermi liquid fits to the data with the parameters discussed in the text. The inset shows a portion of the Brillouin zone with the relevant ellipsoidal electron pocket.

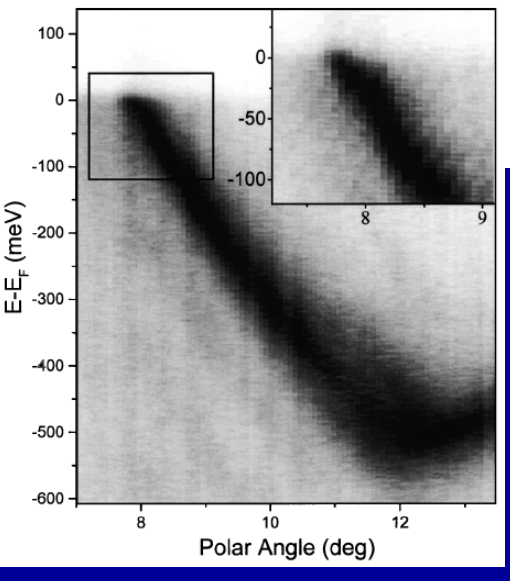

FIG. 1. ARPES intensity plot of the Mo(110) surface recorded along the $\overline{\Gamma}$-$\overline{N}$ line of the surface Brillouin zone at 70 K. Shown in the inset is the spectrum of the region around k_F taken with special attention to t

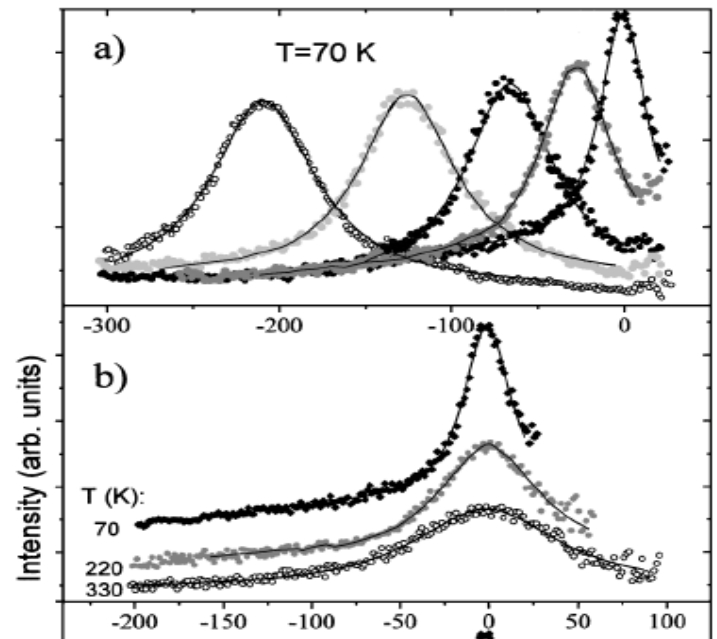

FIG. 2. Spectral intensity as a function of binding energy for constant emission angle, normalized to the experimentally determined Fermi cutoff. Data are symbols, while lines are fits to the Lorentzian peaks with a linear background. The dependence on the (a) binding energy, (b) temperature, and (c) hydrogen exposure is shown.

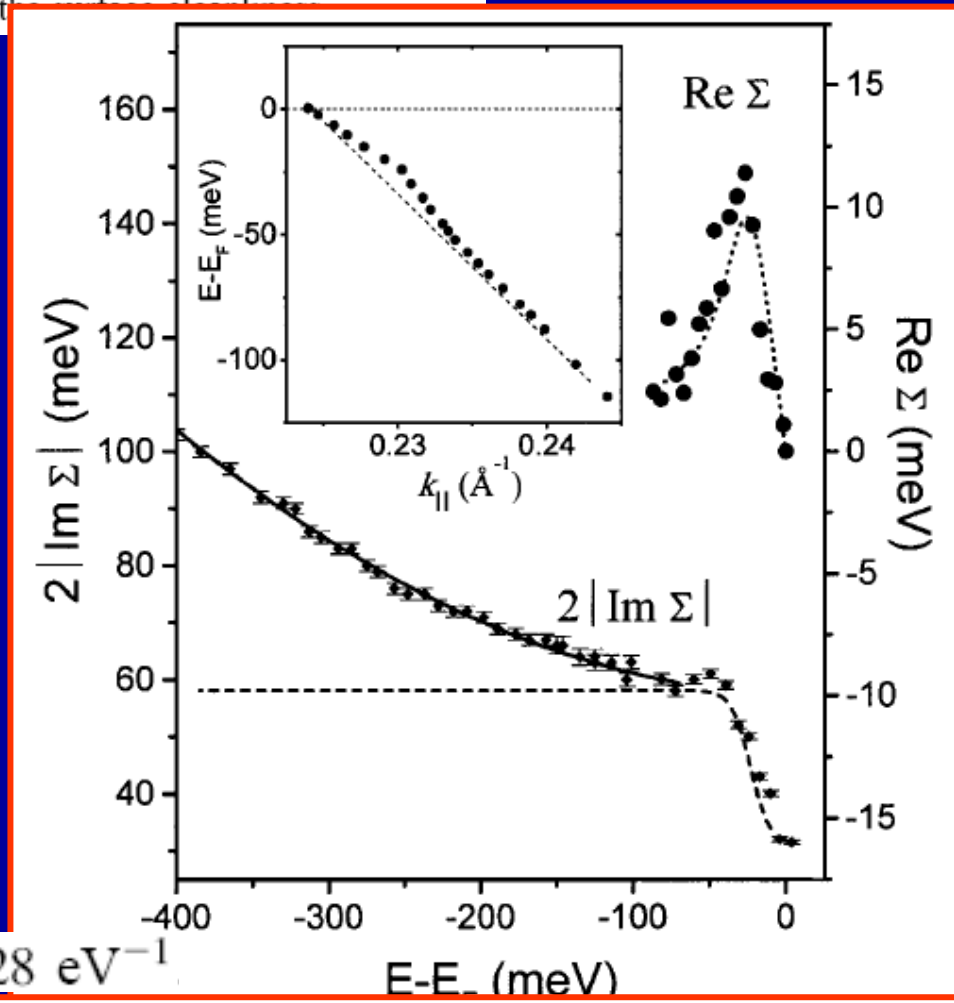

$2\beta \approx 0.28$ eV^{-1}

FIG. 3. The photohole self-energy as a function of binding energy at 70 K. The real part is obtained from the dispersion shown in the inset. The imaginary part is obtained from the width of the quasiparticle peak. The solid line is a quadratic fit to the high-binding energy data ($\omega < -80$ meV). The dashed (dotted) line shows the calculated electron-phonon contribution to the imaginary (real) part of the self-energy. The dashed line is shifted up by 26 meV.

Quasiparticles are destroyed above some *coherence scale* (low in strongly correlated materials)

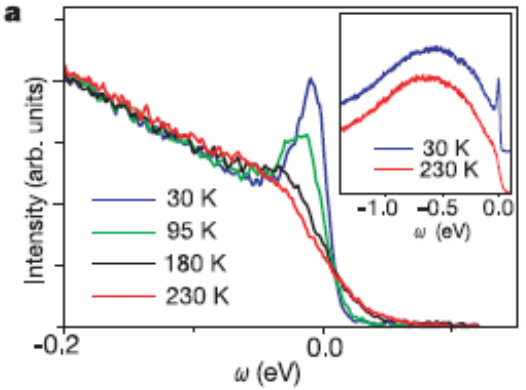

Figure 2 Correlation between the ARPES and transport in $(Bi_{0.5}Pb_{0.5})_2Ba_3Co_2O_y$. **a**, The changes in energy distribution curves (vertical cross-sections of the ARPES data shown in Fig. 1) (for $k = k_F$) with temperature. The inset shows the wide-range energy distribution curves. **b**, Transport data. The in-plane and the out-of-plane resistivities are measured on a sample from the same batch with a conventional four-probe technique.

T.Valla et al. Nature 417 (2002) 628

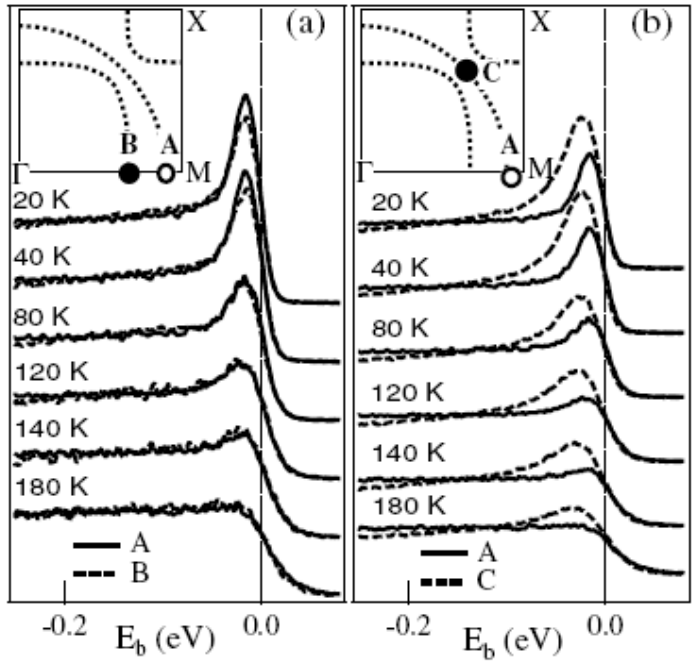

FIG. 2. Temperature dependence of spectra at the three FSCPs: *A*, *B*, and *C* (see the insets). (a) Comparison of spectra between *A* and *B*. (b) Comparison of spectra between *A* and *C*. The insets show measurement locations in the Brillouin zone.

Wang et al PRL 92 (2004) 137002

Fermi liquids with a single scale ?